Electron correlation in FeSe superconductor studied by bulk-sensitive photoemission spectroscopy

A. Yamasaki,[1] Y. Matsui,[1] S. Imada,[2] K. Takase,[3] H. Azuma,[3] T. Muro,[4] Y. Kato,[4, *]

A. Higashiya,[5, †] A. Sekiyama,[6] S. Suga,[6] M. Yabashi,[4] K. Tamasaku,[5] T. Ishikawa,[5] K. Terashima,[2]

H. Kobori,[1] A. Sugimura,[1] N. Umeyama,[7, 8] H. Sato,[9] Y. Hara,[10] N. Miyakawa,[7] and S. I. Ikeda[8]

[1]*Faculty of Science and Engineering, Konan University, Kobe 658-8501, Japan*
[2]*College of Science and Engineering, Ritsumeikan University, Kusatsu 525-8577, Japan*
[3]*College of Science and Technology, Nihon University, Chiyoda, Tokyo 101-8308, Japan*
[4]*Japan Synchrotron Research Institute, Sayo, Hyogo 679-5198, Japan*
[5]*RIKEN, Mikazuki, Sayo, Hyogo 679-5148, Japan*
[6]*Graduate School of Engineering Science, Osaka University, Toyonaka, Osaka 560-8531, Japan*
[7]*Department of Applied Physics, Tokyo University of Science, Shinjuku, Tokyo 162-8601, Japan*
[8]*Nanoelectronics Research Institute, AIST, Tsukuba 305-8568, Japan*
[9]*Faculty of Science and Engineering, Chuo University, Bunkyo, Tokyo 112-8551, Japan*
[10]*Ibaraki National College of Technology, Hitachinaka 312-8508, Japan*
(Dated: September 29, 2010)

We have investigated the electronic structures of recently discovered superconductor FeSe by soft-x-ray and hard-x-ray photoemission spectroscopy with high bulk sensitivity. The large Fe $3d$ spectral weight is located in the vicinity of the Fermi level (E_F), which is demonstrated to be a coherent quasi-particle peak. Compared with the results of the band structure calculation with local-density approximation, Fe $3d$ band narrowing and the energy shift of the band toward E_F are found, suggesting an importance of the electron correlation effect in FeSe. The self energy correction provides the larger mass enhancement value ($Z^{-1} \simeq 3.6$) than in Fe-As superconductors and enables us to separate a incoherent part from the spectrum. These features are quite consistent with the results of recent dynamical mean-field calculations, in which the incoherent part is attributed to the lower Hubbard band.

I. INTRODUCTION

Fe-based high-T_c superconductors have attracted enormous attention for their possibly new-type superconducting mechanism and the potential of breaking the deadlock in the high-T_c superconductor research field. A fluorine doped LaFeAsO has been discovered to be a superconductor below T_c= 26 K, which contains the two dimensional Fe plane in the Fe_2As_2 layer.[1] So far, several tens of superconductors in limited types of mother materials such as LaFeAsO, $BaFe_2As_2$, and LiFeAs, have been synthesized.[2] In addition, a simple Fe-Se binary compound ($FeSe_{0.82}$) has been discovered to show superconductivity.[3] The appearance of superconductivity in the FeSe system indicates Fe_2X_2 (X=P, As, and Se) layer is essential for the superconductivity in these Fe-based superconductors. The density functional study has pointed out that FeSe is not a conventional electron-phonon superconductor, being similar to $LaFeAsO_{1-x}F_x$ system.[4] Other common features to the Fe-based superconductors have also been revealed, which both the antiferromagnetic spin fluctuation and the anion height are closely related to the appearance of the superconductivity.[5,6]

There are, however, many differences between FeSe and other Fe-based superconductors: in FeSe (i) there is no separating layer and the Fe_2Se_2 layer is electrically neutral, (ii) the superconductivity is very sensitive to the deviation from the stoichiometric composition,[7,8]

(iii) there is no magnetically ordered state in p-T phase diagram.[9] Furthermore, it is pointed out by theoretical studies that the electron correlation effect in FeSe is stronger than other Fe-based superconductors.[10,11] In FeSe, only a few experimental results, for instance, Sommerfeld coefficient γ (= 5.4-9.1 mJ/mol K^2) have been so far reported[3,7] although the electron correlation effect in other Fe-based superconductors was investigated by spectroscopic experiments in detail.[12–15]. The reason why no angle-resolved photoemission spectroscopy experiment has been reported to quantitatively evaluate the electron correlation effect in FeSe is that a high quality single crystal is difficult to be grown. Recently, Fe(Se,Te) system has been intensively investigated due to the success of the high-quality single crystal growth. Even so, the Fe(Se, Te) system is essentially different from the end member FeSe in the sense that the magnetically ordered state and remarkably large γ value (= 39 mJ/mol K^2) have been found.[16,17]

We have examined two different synthesis processes for the FeSe superconductor and performed the soft-x-ray and hard-x-ray photoemission spectroscopy (SXPES and HAXPES) in order to quantitatively evaluate the electron correlation effect in the bulk. The SXPES and HAXPES have been widely recognized as the powerful techniques which can reveal bulk electronic structures due to the long inelastic mean free path of photoelectrons excited by high-energy x ray.[18–22] It is found in the

angle-integrated PES spectrum that a large Fe $3d$ spectral weight is located in the vicinity of the Fermi level (E_F) and it decreases steeply toward E_F, being a similar feature to those in the other Fe-based superconductors non-doped LaFePO and LaFePnO$_{0.94}$F$_{0.06}$ (Pn=P, As).[12,23] Considering the self energy correction to the results of band structure calculations, the experimentally observed band narrowing and the energy shift of the band toward E_F are fully explained. The correction also provides the renormalization factor Z of $\simeq$0.28 and enables us to separate the incoherent part of the quasi-particle spectrum.

II. EXPERIMENTAL

For SXPES and HAXPES measurements, single-crystalline tetragonal [Tet(Single)] FeSe and polycrystalline tetragonal [Tet(Poly)] FeSe were employed, together with polycrystalline hexagonal [Hex(Poly)] FeSe (likely, Fe$_7$Se$_8$) as a reference material.[7] The Tet(Single) FeSe was grown by the chemical vapor transport method using Fe and Se powders.[24] It was found to contain the hexagonal phase around the crystal edge by x-ray powder diffraction (XRD) measurements. The coexistence of two stable phases has also been reported by other groups.[7,25–27] The spot size of the SX beam in PES measurements is small ($\sim 10\mu$m $\times 100\mu$m) enough to exclude signals from the hexagonal phase near the crystal edge because of the much larger sample size ($\sim 500\mu$m $\times 500\mu$m). The Tet(Poly) FeSe was synthesized using a high-frequency induction furnace. The furnace is very useful for quick cooling of the samples because this furnace can heat only the samples. This makes the pass time through other low temperature phase relatively short. The Hex(Poly) FeSe was prepared by a conventional solid state reaction. Crystal structures of both the Tet(Poly) and Hex(Poly) FeSe were also evaluated by XRD. The Rietveld analysis against the XRD profiles reveals that the Tet(Poly) FeSe sample contains the hexagonal-phase FeSe of 10% as an impurity and the Hex(Poly) FeSe sample has a single phase with in the limits of the resolution. The Tet(Single) FeSe and Tet(Poly) FeSe have the transition temperature $T_c^{\text{zero}} \simeq$6 K estimated by $\rho-T$ and $T_c \simeq$8 K estimated by $\chi-T$ measurements under ambient pressure, respectively, which are similar to reported values.[3,7,25] This implies the present samples have the selenium defect of few percent.

SXPES was carried out at both the Figure-8 undulator SX beamline BL27SU in SPring-8 using the SPECS PHOIBOS 150 hemispherical electron energy analyzer and the twin-helical undulator SX beamline BL25SU in SPring-8 using GAMMADATA-SCIENTA SES-200 spectrometer.[28,29] The highest total energy resolution ΔE [the full width at half maximum (FWHM)] was set to 75 meV at hν=600 eV. HAXPES was performed at the beamline BL19LXU in SPring-8 with MB Scientific A1-HE spectrometer. The linearly polarized light was de-
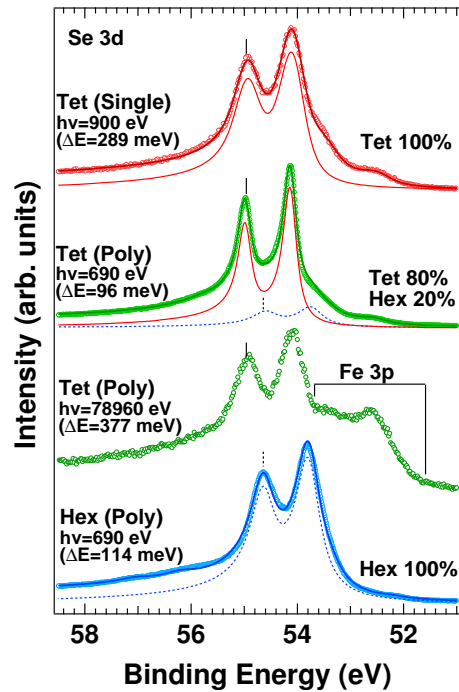

FIG. 1: (Color online) Se $3d$ core-level PES spectra of FeSe. Circles and thick solid curve indicate the experimental and fitted spectra, respectively. The Se $3d$ components of tetragonal and hexagonal phases are shown by thin solid and broken curves. The other components, for instance, Fe $3p$ and background are not displayed for simplicity.

livered from an in-vacuum 27 m long undulator.[30] The ΔE for the valence-band PES spectrum near E_F was set to $\sim$380 meV at h$\nu \simeq$8 keV. Clean surfaces of the samples were obtained by fracturing samples *in situ* in UHV ($\sim$4$\times10^{-8}$ Pa) at the measuring temperature ($T \simeq$20 K).

III. RESULTS AND DISCUSSION

FeSe has two stable crystal phases, that is, the tetragonal and the hexagonal phases and often contains both in one sample as has been mentioned above. In order to investigate the crystal phase mixing in samples, Se $3d$ (including Fe $3p$) core-level PES spectra were measured for Tet(Single), Tet(Poly), and Hex(Poly) FeSe samples. The Se $3d$ core-level PES spectra in both crystal phases excited by SX have a sharp doublet peak structure originating from Se $3d_{5/2}$ and $3d_{3/2}$ components as shown in Fig. 1. There is no surface-derived peak and only weak plasmon satellites are seen on the higher binding energy (E_B) side of the Se $3d$ peaks, indicating that the surface contributions to the spectra can be ruled out in the SXPES for the shallow core levels (including the valence band) for FeSe. In addition, the spectra in the tetragonal FeSe have the shoulder structure on the lower E_B side, which originates from the Fe $3p$ states. In the HAXPES the intensity of the shoulder is enhanced since the pho-
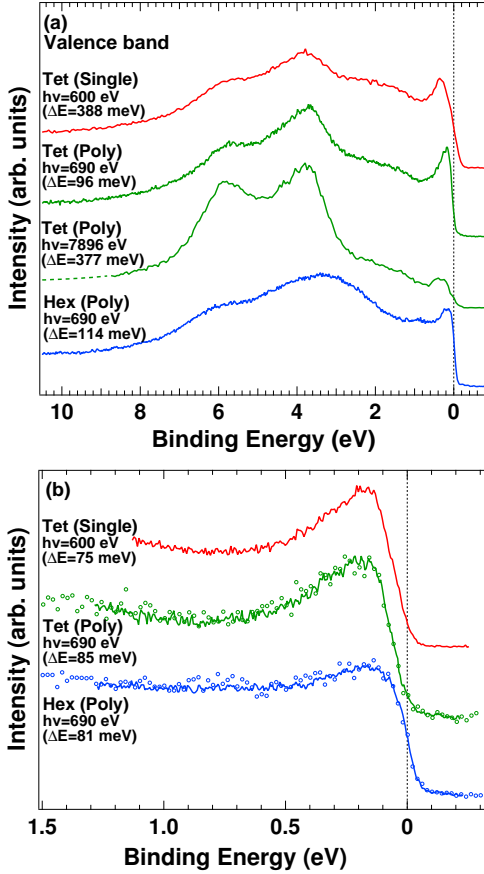
FIG. 2: (Color online) Valence-band PES spectra of FeSe. (a) Overall valence-band SXPES and HAXPES spectra. These spectra are normalized by the area under the curves after subtracting the Shirley-type background.[33] (The dotted line indicates the extrapolated one assuming the Lorentzian line shape in order to normalize the HAXPES spectrum.) (b) High-resolution PES spectra near E_F. The spectra of polycrystalline samples are normalized so that the spectral intensity agrees with the intensity in each normalized high-resolution overall valence-band PES spectrum (shown partly by dots).

FIG. 3: (Color online) Fe $2p$ core-level SXPES and HAXPES spectra of FeSe.

toionization cross section σ of Fe $3p$ states relative to that of Se $3d$ states increases by a factor of 8 compared with the SXPES.[31] We have obtained the tetragonal and/or hexagonal components in each sample by a deconvolution procedure.[32] The Se $3d$ peaks in the tetragonal and hexagonal components are located at the certain energies in these samples, respectively, as shown by solid and dotted bars in Fig. 1. The peak of the tetragonal component is located at the E_B which is about 300 meV higher than that of the hexagonal one. This shift is caused by the structural difference, in other words, the difference of the covalent bond strength between these compounds, being consistent with what Se $4p$ states have a different structure in the valence band of these compounds (discussed later). We note that the Tet(Poly) FeSe has the hexagonal component of 20 % in the Se $3d$ core-level PES spectrum. The influence of the hexagonal FeSe inclusion
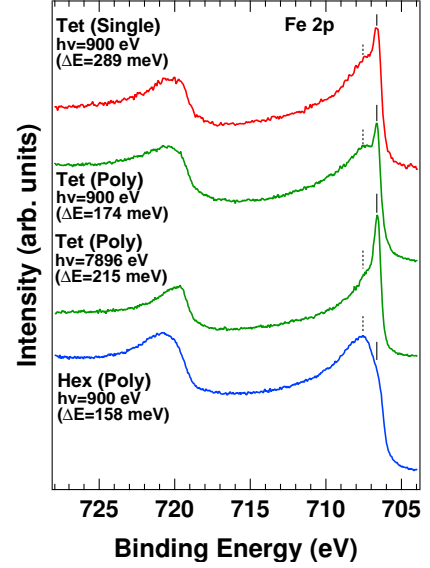
on other spectra of Tet(Poly) FeSe will be discussed later.

Figure 2 (a) shows valence-band SXPES and HAXPES spectra of the tetragonal and hexagonal FeSe. In both the tetragonal and hexagonal FeSe the SXPES spectra have a sharp peak in the vicinity of E_F. In addition, there are some broad peaks and hump structures in the higher E_B region. The spectra of the tetragonal FeSe have the features very similar to the recently reported result.[34] These structures consist of Fe $3d$ and Se $4p$ states as has been revealed later by comparison with theoretical spectra. In the HAXPES spectrum, it is found that the peak near E_F is suppressed and the structures in the E_B=3-7 eV become dominant. Such a variation of the spectral shape in the SXPES and HAXPES does not mainly originate from the increase of the bulk sensitivity but from the ratio of σ between Fe $3d$ and Se $4p$ states, that is, Fe$(3d)$/Se$(4p)$ is 2.8 at h$\nu \simeq$690 eV and 0.033 at $\simeq$8 keV. This indicates that the HAXPES spectrum of the valence band is nearly equivalent to the Se $4p$ (including weak and broad s) states.

Now we focus on the similarity and difference of the electronic structures between the tetragonal and hexagonal FeSe. They have rather different Se $4p$ electronic structures between E_B= 3 eV and 5 eV as recognized in Fig. 2 (a). Furthermore, high-resolution PES spectra reveal that Fe $3d$ states near E_F also have different features as shown in Fig. 2 (b). We note that each spectrum of Tet(Poly) and Hex(Poly) FeSe is normalized by the integrated intensity of its high-resolution whole valence-band PES spectrum after subtracting the background. The Tet(Poly) FeSe has a prominent peak at $E_B \simeq$ 180 meV. The photoemission intensity decreases steeply toward E_F and is very weak at E_F. Meanwhile, the Hex(Poly) FeSe has a less prominent peak, which is closer to E_F. In
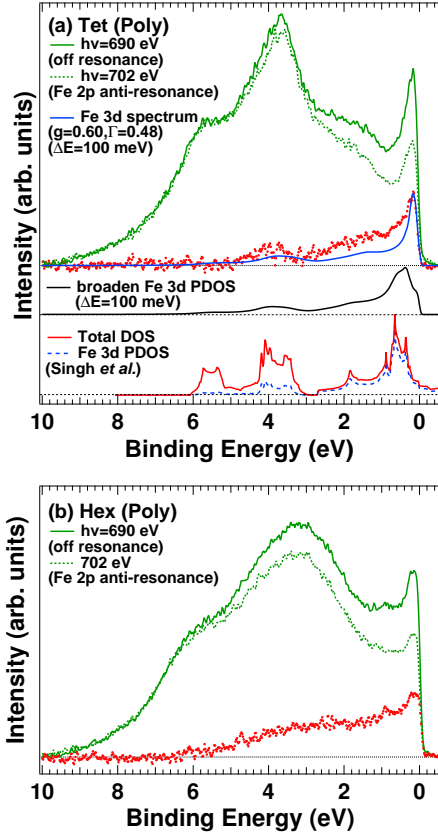
FIG. 4: (Color online) Valence-band PES spectra of FeSe measured at two different photon energies. The spectrum indicated by dots is difference between the off-resonance (measured at hν=690 eV) and anti-resonance (measured at hν=702 eV) spectra for (a) tetragonal FeSe and (b) hexagonal FeSe. In the middle of Figure (a), calculated Fe 3d spectrum including the self energy correction and the broadened Fe 3d PDOS are shown by solid lines. The original DOSs calculated by Singh *et al.* are also shown.[4]

FIG. 5: (Color online) High-resolution PES spectra near E_F. (a) The broken lines indicate the calculated Fe 3d spectrum (blue) and Fe 3d PDOS (black) without broadening and finite temperature effects. Other explanations are the same as in Fig.4 (a). (b) The PES spectrum measured at hν=40 eV. The calculated Fe3d spectrum without broadening is also shown.

addition, the obvious Fermi cut off is observed in the Hex(Poly) FeSe. Here we would stress that the spectra near E_F in the Tet(Single) FeSe is in good agreement with in the Tet(Poly) FeSe, indicating that the influence of the hexagonal FeSe inclusion in Tet(Poly) FeSe is negligible near E_F.

Fe 2p core-level PES spectra of the tetragonal and hexagonal FeSe are shown in Fig. 3. There is no charge-transfer satellite, as has been pointed out in LaFeAsO.[23] In addition, one can see the sharp-peak-and-shoulder structure in the $2p_{3/2}$ component of the SXPES spectra of both the Tet(Single) and Tet(Poly) FeSe as indicated by solid and dotted bars. Considering that the sharp peak becomes more prominent in the HAXPES spectrum, the peak can be assigned to the bulk $|2p^5 3d^6\rangle$ component. The sharp peak structure suggests the existence of the highly coherent valence electrons in the bulk. Then, the shoulder structure is attributed to the photoe-
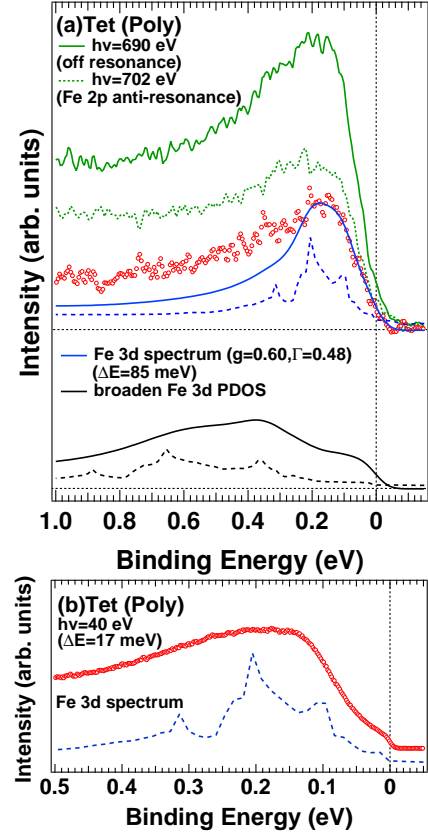
mission from the surface (and grain boundaries in the polycrystalline sample). These indicate that the photo-electrons with the low E_K (of less than a few hundred eV) lead to the large surface contribution to the spectrum even in the SXPES experiment.[35] The possibility cannot be ruled out that the slightly stronger shoulder intensity in the SXPES spectrum of Tet(Poly) FeSe than that of Tet(Single) FeSe originates from the influence of the hexagonal FeSe inclusion. Meanwhile, the Hex(Poly) FeSe has a broad peak originating from multiplet structures. The overall spectral shape is very similar to the reported spectrum in the hexagonal Fe_7Se_8.[36]

Let us discuss Fe 3d states in the valence band PES spectra of the tetragonal and hexagonal FeSe. In Fig. 4 (a), the valence-band PES spectra of the Tet(Poly) FeSe measured at two different photon energies are shown. The solid line indicates the spectrum obtained at hν=690 eV, which is labeled as "off-resonance" in comparison to another spectrum. The dotted line shows the spectrum which was measured at the energy just below the threshold of Fe 2p-3d absorption edge, labeled as "Fe 2p anti-resonance". In this spectrum Fe 3d states are

strongly suppressed since the tuned photon energy corresponds to the energy providing the mostly minimum transition probability in the Fano lineshape.[37] One can see that the spectral weight between E_F and E_B=3 eV is remarkably reduced. This indicates Fe $3d$ dominant states are located in this E_B range. However, some spectral weights still remain, suggesting that there are Se $4p$ states hybridized with the Fe $3d$ states as seen in the HAXPES spectrum of Fig. 2 (a). Meanwhile, no significant reduction above E_B=3 eV is seen except for the slight decrease around E_B=4 eV, since these structures mainly originate from Se $4p$ states. We note that one often employs the (on-) resonant PES to investigate the contribution of the specific electronic states by using the photon energy tuned to the core-level absorption maximum. In the present case, however, the Auger decay process becomes dominant and the valence-band structures are smeared out due to the large background. The difference spectrum between the off-resonance (hν=690 eV) and anti-resonance spectra is also shown as dots in Fig. 4 (a), which represents the Fe $3d$ partial density of states (PDOS) if the electron correlation effect is negligible. It has a sharp peak in the vicinity of E_F and broad hump structures at around E_B=1.5 eV and 4 eV. The difference spectrum has similar features to the experimentally obtained Fe $3d$ states of LaFePnO$_{0.94}$F$_{0.06}$ (Pn=P, As).[23] Meanwhile, the Hex(Poly) FeSe has much different Fe $3d$ states from the Tet(Poly) FeSe as shown in Fig. 4 (b). The difference spectrum has a large spectral weight up to E_B=6 eV and broad hump structure around 3 eV. These features are consistent with those in Fe$_7$Se$_8$ spectrum measured at hν=100 eV.[36] The SX spectrum has a stronger peak near E_F than the lower-hν spectrum presumably due to the high bulk sensitivity.[19]

The results of the band structure calculations with the local-density approximation (LDA) for the tetragonal FeSe done by Singh et $al.$ and the Fe $3d$ PDOS broadened by Gaussian and Lorentzian functions representing the experimental energy resolution and the lifetime broadening effect are also shown in the Fig. 4 (a). By comparison with them, narrowing the Fe $3d$ band width and the energy shift of the band toward E_F are found in the difference spectrum of the Tet(Poly) FeSe, suggesting that the electron correlation effect cannot be negligible to discuss the electronic structures in this system. In order to take into account the electron correlation effect quantitatively, the self energy $\Sigma(\boldsymbol{k},\omega)$ defined as $\Sigma(\boldsymbol{k},\omega) \equiv G_0^{-1}(\boldsymbol{k},\omega) - G^{-1}(\boldsymbol{k},\omega)$ is often employed, where $G_0(\boldsymbol{k},\omega)$ and $G(\boldsymbol{k},\omega)$ are the one-electron Green's functions without and with the electron-electron interaction. We have calculated the spectrum with the self energy correction in accordance with the procedure reported by Shimada et $al.$[36] The $\boldsymbol{k}$-independent self energy is assumed to be given by $\Sigma(\omega) = g\omega/(\omega + i\Gamma)^2$, where g and Γ are employed as fitting parameters and $\hbar\omega < \mu(= 0)$ for the occupied state. The $\boldsymbol{k}$-integrated one-particle spectral function for Fe $3d$ states including the electron-electron interaction, hereafter called "Fe $3d$

spectrum" $A_d(\omega)$, is obtained as follows,

$$A_d(\omega) = \sum_{\boldsymbol{k}} A_d(\boldsymbol{k}, \omega) \tag{1}$$

$$= -\frac{1}{\pi} \sum_{\boldsymbol{k}} \int_{-\infty}^{+\infty} d\epsilon_{\boldsymbol{k}}^0 D_d(\epsilon_{\boldsymbol{k}}^0) \mathrm{Im} G(\boldsymbol{k}, \omega)$$

$$= -\frac{1}{\pi} \sum_{\boldsymbol{k}} \int_{-\infty}^{+\infty} d\epsilon_{\boldsymbol{k}}^0 \Bigg[D_d(\epsilon_{\boldsymbol{k}}^0)$$

$$\times \frac{\mathrm{Im}\Sigma(\boldsymbol{k}, \omega)}{\{\hbar\omega - \epsilon_{\boldsymbol{k}}^0 - \mathrm{Re}\Sigma(\boldsymbol{k}, \omega)\}^2 + \{\mathrm{Im}\Sigma(\boldsymbol{k}, \omega)\}^2} \Bigg],$$

where $D_d(\epsilon_{\boldsymbol{k}}^0)$ denotes Fe $3d$ PDOS. The obtained spectrum after optimizing the parameters (g=0.60, Γ=0.48) is shown in Fig. 4 (a), which includes the broadening and finite temperature effects. The calculated Fe $3d$ spectrum has the peak near E_F as a coherent quasi-particle peak, which becomes much sharper than in the PDOS without the electron correlation effect, and has two broad hump structures at around 2 and 4 eV. Thus, it reproduces well the overall valence-band features experimentally obtained. The comparison between the experimental and calculated Fe $3d$ states near E_F are shown in Fig. 5. The peak shift of the spectrum toward E_F due to the self-energy correction is obviously seen, the energy of which corresponds to $\mathrm{Re}\Sigma(\omega)$ in the non-broadened spectrum. One can also see that the leading edge behavior in the vicinity of E_F and the peak position is well reproduced. We have measured the further higher-resolutioin spectrum at a low energy excitation (hν=40 eV) shown in Fig. 5 (b). In this photon energy the Fe $3d$-state-dominant spectrum is obtained since the σ of Fe $3d$ states is 16 times larger than that of Se $4p$ states.[31] Although the spectrum should be very sensitive to the surface electronic structures, the spectral features agree well with the calculated Fe $3d$ spectrum.

There is a discrepancy between the experimentally and theoretically obtained Fe $3d$ spectra in the E_B=0.2-3 eV as seen in Fig. 4(a) and Fig 5(a). This should be due to the contribution of the incoherent part of the spectral function, $A_d^{\mathrm{inc}}(\boldsymbol{k}, \omega)$. In the present analysis, only the pole part of the Green's function, that is, the coherent part is considered. Thus, the quasi-particle spectral weight is reduced to $Z_{\boldsymbol{k}}$,

$$\int_{-\infty}^{+\infty} d\omega A_d^{\mathrm{coh}}(\boldsymbol{k}, \omega) = Z_{\boldsymbol{k}} (< 1) \tag{2}$$

where $Z_{\boldsymbol{k}}$ and $A_d^{\mathrm{coh}}(\boldsymbol{k}, \omega)$ are the renormalization factor and the coherent part of the spectral function A_d $(\boldsymbol{k}, \omega)$ for Fe $3d$ states. According to the sum rules of the spectral function, the following spectral weight of the incoherent part remains in the occupied and unoccupied states,

$$\int_{-\infty}^{+\infty} d\omega A_d^{\mathrm{inc}}(\boldsymbol{k}, \omega) = 1 - Z_{\boldsymbol{k}}. \tag{3}$$

The incoherent part should appear at $\hbar\omega \simeq \epsilon_{\boldsymbol{k}}^0 + \mathrm{Re}\Sigma(\omega)$ on the higher E_B side of the quasi-particle peak, for in-

TABLE I: Experimentally and theoretically obtained mass enhancement factor (Z^{-1} or m^*/m_b) for typical Fe-based superconductor systems. † indicates the non-superconductor. The Sommerfeld coefficient γ is also listed.

	LaFePnO	†BaFe$_2$As$_2$	(Ba,K)Fe$_2$As$_2$	FeSe	Fe(Se,Te)
m^*/m_b [PES]	1.5-2.2 (Pn=P), 1.8 (Pn=As, F-doped) Ref.[12,14,23]	1.5 Ref.[13]	2.7 Ref.[13]	3.6	6-20 Ref.[39]
m^*/m_b [DMFT]	1.9-2.2(Pn=P), 1.6 (Pn=†As) Ref.[40,41]	1.8-2.1 Ref.[42]	–	2-5 Ref.[11]	–
γ (mJ/mol K^2)	10.1-12.5(Pn=P) Ref.[43,44]	16-37 Ref.[45,46]	23 Ref.[46]	5.4-9.1 Ref.[3,7]	39 Ref.[16]

stance, $\hbar\omega \simeq 1.0$eV for $\epsilon_{\boldsymbol{k}}^0 \simeq 0.65$ eV in the largest peak of the original Fe 3d PDOS. This is consistent with the energy region in which the disagreement between experimental and calculated spectra are seen. In fact, in very recent articles, theoretical works predict that the incoherent spectral weight appears around $E_B \simeq 2$ eV as a lower Hubbard band.[10,11]

The $Z_{\boldsymbol{k}}^{-1}$ at $k = k_F$, that is, Z^{-1} depends on the real part of the self energy Re$\Sigma(\omega)$ as follows,[38]

$$Z^{-1} \equiv 1 - \left.\frac{\partial \mathrm{Re}\Sigma(\omega)}{\partial \omega}\right|_{\omega=0} = 1 + \frac{g}{\Gamma^2}. \qquad (4)$$

The Z^{-1} represents the mass enhancement due to the band narrowing of the quasi-particle peak. In the present work, we have obtained Z^{-1}=3.6, which is about twice as heavy as the reported values in LaFeAsO$_{0.94}$F$_{0.06}$.[23] In Table I, the obtained Z^{-1}, that is, m^*/m_b (the ratio of the enhanced effective mass to the bare band mass) and some reported values related to the electron correlation in Fe-based superconductor systems are summarized. Spectroscopic and theoretical studies clearly indicates the common tendency of the electron correlation strength in these systems, that is, stronger on the right side, although the γ value in FeSe is peculiarly smaller than in other superconductors. We conclude that the electron correlation in the FeSe superconductor is relatively strong, being quantitatively consistent with the results of the DFT +DMFT (the density-functional theory combined with the dynamical mean-field theory) study.[11]

IV. SUMMARY

We have performed the bulk-sensitive SXPES and HAXPES for Fe-based superconductor FeSe. It is suggested in the Fe 2p core-level PES that the tetragonal FeSe has the Fe 3d electrons with the highly coherent character unlike the non-superconducting FeSe with the hexagonal structure. In comparison to the results of band structure calculations, the Fe 3d band narrowing and its energy shift are revealed, which originates from the electron correlation effect. Considering the self energy correction, the larger mass enhancement ($Z^{-1} \simeq 3.6$) than in other Fe-As superconductors are obtained. In addition, the incoherent part of the quasi-particle spectrum are found and successfully separated. The obtained mass enhancement value and the energy position of the incoherent part are consistent with the results of recent dynamical mean-field calculations.

* Present address : Diamond Research Laboratory, AIST, Tsukuba 305-8568, Japan
† Present address : Industrial Technology Center of Wakayama Prefecture, Wakayama 649-6261, Japan
[1] Y. Kamihara, T. Watanabe, M. Hirano, and H. Hosono, J. Am. Chem. Soc. **130**, 3296 (2008).

[2] M. R. Norman, Physics **1**, 21 (2008), and references therein.

[3] F. C. Hsu, J. Y. Luo, K. W. Yeh, T. K. Chen, T. W. Huang, P. M. Wu, Y. C. Lee, Y. L. Huang, Y. Y. Chu, D. C. Yan, and M. K. Wu, Proc. Natl. Acad. Sci. U.S.A. **105**, 14262 (2008).

[4] A. Subedi, L. Zhang, D. J. Singh, and M. H. Du, Phys. Rev. B **78**, 134514 (2008).

[5] T. Imai, K. Ahilan, F. L. Ning, T. M. McQueen, and R. J. Cava, Phys. Rev. Lett. **102**, 177005 (2009).

[6] H. Okabe, N. Takeshita, K. Horigane, T. Muranaka, and J. Akimitsu, Phys. Rev. B **81**, 205119 (2010).

[7] T. M. McQueen, Q. Huang, V. Ksenofontov, C. Felser, Q. Xu, H. Zandbergen, Y. S. Hor, J. Allred, A. J. Williams, D. Qu, J. Checkelsky, N. P. Ong, and R. J. Cava, Phys. Rev. B **79**, 014522 (2009).

[8] E. Pomjakushina, K. Conder, V. Pomjakushin, M. Bendele, and R. Khasanov, Phys. Rev. B **80**, 024517 (2009).

[9] S. Medvedev, T. M. McQueen, I. A. Troyan, T. Palasyuk, M. I. Eremets, R. J. Cava, S. Naghavi, F. Casper, V. Ksenofontov, G.Wortmann, and C. Felser, Nature Mater. **14**, 630 (2009).

[10] T. Miyake, K. Nakamura, R. Arita, and M. Imada, J. Phys. Soc. Jpn. **79**, 044705 (2010).

[11] M. Aichhorn, S. Biermann, T. Miyake, A. Georges, and M. Imada, Phys. Rev. B **82**, 064504 (2010).

[12] D. H. Lu, M. Yi, S.-K. Mo, A. S. Erickson, J. Analytis, J.-H. Chu, D. J. Singh, Z. Hussain, T. H. Geballe, I. R. Fisher, and Z.-X. Shen, Nature (London) **455**, 81 (2008).

[13] M. Yi, D. H. Lu, J. G. Analytis, J.-H. Chu, S.-K. Mo, R.-H. He, R. G. Moore, X. J. Zhou, G. F. Chen, J. L. Luo, N. L. Wang, Z. Hussain, D. J. Singh, I. R. Fisher, and Z.-X. Shen, Phys. Rev. B **80**, 024515 (2009).

[14] M. M. Qazilbash, J. J. Hamlin, R. E. Baumbach, L. Zhang, D. J. Singh, M. B. Maple, and D. N. Basov, Nature Phys. **5**, 647 (2009).

[15] W. L. Yang, A. P. Sorini, C-C. Chen, B. Moritz, W.-S. Lee, F. Vernay, P. Olalde-Velasco, J. D. Denlinger, B. Delley, J.-H. Chu, J. G. Analytis, I. R. Fisher, Z. A. Ren, J. Yang, W. Lu, Z. X. Zhao, J. van den Brink, Z. Hussain, Z.-X. Shen, and T. P. Devereaux, Phys. Rev. B **80**, 014508 (2009).

[16] B. C. Sales, A. S. Sefat, M. A. McGuire, R. Y. Jin, and D. Mandrus, Phys. Rev. B **79**, 094521 (2009).

[17] R. Khasanov, M. Bendele, A. Amato, P. Babkevich, A. T. Boothroyd, A. Cervellino, K. Conder, S. N. Gvasaliya, H. Keller, H.-H. Klauss, H. Luetkens, V. Pomjakushin, E. Pomjakushina, and B. Roessli, Phys. Rev. B **80**, 140511R (2009).

[18] E. Weschke, C. Laubschat, T. Simmons, M. Domke, O. Strebel, and G. Kaindl, Phys. Rev. B **44**, 8304 (1991).

[19] A. Sekiyama, T. Iwasaki, K. Matsuda, Y. Saitoh, Y. Ōnuki, and S. Suga, Nature (London) **403**, 396 (2000); A. Sekiyama, K. Kadono, K. Matsuda, T. Iwasaki, S. Ueda, S. Imada, S. Suga, R. Settai, H. Azuma, Y. Ōnuki, and Y. Saitoh, J. Phys. Soc. Jpn. **69**, 2771 (2000).

[20] S.-K. Mo, J. D. Denlinger, H.-D. Kim, J.-H. Park, J.W. Allen, A. Sekiyama, A. Yamasaki, K. Kadono, S. Suga, Y. Saitoh, T. Muro, P. Metcalf, G. Keller, K. Held, V. Eyert, V. I. Anisimov, and D. Vollhardt, Phys. Rev. Lett. **90**, 186403 (2003).

[21] A. Yamasaki, S. Imada, T. Nanba, A. Sekiyama, H. Sugawara, H. Sato, C. Sekine, I. Shirotani, H. Harima, and S. Suga, Phys. Rev.B **70**, 113103 (2004); A. Yamasaki, S. Imada, H. Higashimichi, H. Fujiwara, T. Saita, T. Miyamachi, A. Sekiyama, H. Sugawara, D. Kikuchi, H. Sato, A. Higashiya, M. Yabashi, K. Tamasaku, D. Miwa, T. Ishikawa, and S. Suga, Phys. Rev. Lett. **98**, 156402 (2007).

[22] A. Sekiyama, S. Imada, A. Yamasaki, and S. Suga, *Very High Resolution Photoelectron Spectroscopy*, edited by S. Hüfner, Lect. Notes. Phys. **715** (Springer, Berlin Heidelberg 2007), p. 367.

[23] W. Malaeb, T. Yoshida, T. Kataoka, A. Fujimori, M. Kubota, K. Ono, H. Usui, K. Kuroki, R. Arita, H. Aoki, Y. Kamihara, M. Hirano, and H. Hosono, J. Phys. Soc. Jpn. **77**, 093714 (2008).

[24] Y. Hara, K. Takase, A. Yamasaki, H. Sato, N. Miyagawa, N. Umeyama, and S. Ikeda, Physica C (in press).

[25] Y. Mizuguchi, F. Tomioka, S. Tsuda, T. Yamaguchi, and Y. Takano, Appl. Phys. Lett. **93**, 152505 (2008).

[26] S. B. Zhang, Y. P. Sun, X. D. Zhu, X. B. Zhu, B. S. Wang, G. Li, H. C. Lei, X. Luo, Z. R. Yang, W. H. Song, and J. M. Dai, Supercond. Sci. Technol. **22**, 015020 (2009).

[27] M. Bendele, S. Weyeneth, R. Puzniak, A. Maisuradze, E. Pomjakushina, K. Conder, V. Pomjakushin, H. Luetkens, S. Katrych, A. Wisniewski, R. Khasanov, and H. Keller, Phys. Rev. B **81**, 224520 (2010).

[28] H.Ohashi, E. Ishiguro, Y. Tamenori, H. Okumura, A. Hiraya, H. Yoshida, Y. Senba, K. Okada, N. Saito, I. H. Suzuki, K. Ueda, T. Ibuki, S. Nagaoka, I. Koyano, and T. Ishikawa, Nucl. Instrum. Meth. A **467-468**, 533 (2001).

[29] Y. Saitoh, H. Kimura, Y. Suzuki, T. Nakatani, T. Matsushita, T. Muro, T. Miyahara, M. Fujisawa, K. Soda, S. Ueda, H. Harada, M. Kotsugi, A. Sekiyama, and S. Suga, Rev. Sci. Instrum. **71**, 3254 (2000).

[30] M. Yabashi, K. Tamasaku, and T. Ishikawa, Phys. Rev. Lett. **87**, 140801 (2001).

[31] J. J. Yeh and I. Lindau, At. Data Nucl. Data Tables **32**, 1 (1985).

[32] A. Sekiyama, S. Kasai, M. Tsunekawa, Y. Ishida, M. Sing, A. Irizawa, A. Yamasaki, S. Imada, T. Muro, Y. Saitoh, Y. Onuki, T. Kimura, Y. Tokura, and S. Suga, Phys. Rev. B **70**, 060506R (2004).

[33] D. A. Shirley, Phys. Rev. B **5**, 4709 (1972).

[34] R. Yoshida, T. Wakita, H. Okazaki, Y. Mizuguchi, S. Tsuda, Y. Takano, H. Takeya, K. Hirata, T. Muro, M. Okawa, K. Ishizaka, S. Shin, H. Harima, M. Hirai, Y. Muraoka, and T. Yokoya, J. Phys. Soc. Jpn. **78**, 034708 (2009).

[35] S. Tanuma, C. J. Powell, and D. R. Penn, Surf. Interface anal. **21**, 165 (1994).

[36] K. Shimada, T. Mizokawa, K. Mamiya, T. Saitoh, A. Fujimori, K. Ono, A. Kakizaki, T. Ishii, M. Shirai, and T. Kamimura, Phys. Rev. B **57**, 8845 (1998).

[37] U. Fano, Phys. Rev. **124**, 1866 (1961).

[38] M. Imada, A. Fujimori, and Y. Tokura, Rev. Mod. Phys. **70**. 1039 (1998).

[39] A. Tamai, A.Y. Ganin, E. Rozbicki, J. Bacsa, W. Meevasana, P. D. C. King, M. Caffio, R. Schaub, S. Margadonna, K. Prassides, M. J. Rosseinsky, and F. Baumberger, Phys. Rev. Lett. **104**, 097002 (2010).

[40] M. Aichhorn, L. Pourovskii, V. Vildosola, M. Ferrero, O. Parcollet, T. Miyake, A. Georges, and S. Biermann, Phys. Rev. B **80**, 085101 (2009).

[41] S. L. Skornyakov, N. A. Skorikov, A. V. Lukoyanov, A. O. Shorikov, and V. I. Anisimov, Phys. Rev. B **81**, 174522 (2010).

[42] S. L. Skornyakov, A. V. Efremov, N. A. Skorikov, M.

A. Korotin, Yu. A. Izyumov, V. I. Anisimov, A. V. Kozhevnikov, and D. Vollhardt, Phys. Rev. B **80**, 092501 (2009).

[43] S. Suzuki, S. Miyasaka, S. Tajima, T. Kida, and M. Hagiwara, J. Phys. Soc. Jpn. **78**, 114712 (2009).

[44] T. M. McQueen, M. Regulacio, A. J. Williams, Q. Huang, J. W. Lynn, Y. S. Hor, D. V. West, M. A. Green, and R. J. Cava, Phys. Rev. B **78**, 024521 (2008).

[45] M. Rotter, M. Tegel, D. Johrendt, I. Schellenberg, W. Hermes, and R.Pöttgen, Phys. Rev. B **78**, 020503R (2008).

[46] N. Ni, S. L. Bud'ko, A. Kreyssig, S. Nandi, G. E. Rustan, A. I. Goldman, S. Gupta, J. D. Corbett, A. Kracher, and P. C. Canfield, Phys. Rev. B **78**, 014507 (2008).